Using Integral and Differential Charge Asymmetries for BSM Searches at the LHC

Steve Muanza
CPPM, CNRS-IN2P3 & AMU, Marseille FRANCE
E-mail: muanza@in2p3.fr

Abstract. Contrarily to past high energy colliders, the LHC is a charge asymmetric machine. Therefore most of the hard scattering processes producing electrically charged final states have a positive integral charge asymmetry. The latter quantity, denoted $A_C(\ell^{\pm})$, is easily measurable in event topologies bearing an odd number of hard and isolated charged leptons. We have brought to light the strong correlation between $A_C(\ell^{\pm})$ and the mass of the charged final state. This enabled us to setup a new method of indirect mass measurement [1]. For example, this method enables to measure the mass of the $W^{\pm}$ boson with a 2% accuracy. Obviously this is not competitive with respect to the standard technique based on the $W^{\pm}$ transverse mass. However for other processes where more final state particles escape detection, we've demonstrated the integral charge asymmetry method to be much more effective. We illustrate this in a search for a supersymmetric production of chargino-neutralino pairs decaying in the trilepton inclusive topology and show that we can measure $M_{\tilde{\chi}_1^{\pm}} + M_{\tilde{\chi}_2^0}$ with an accuracy better than 10%. Nevertheless, in order to apply the integral charge asymmetry method, one needs to have a significant excess of signal events over the event yield of the corresponding background processes. We are currently extending this indirect mass measurement method using differential charge asymmetries. In addition to their sensitivity to the mass, the shape of these observables can also be exploited to improve the separation between a signal and its background processes. Our main physics case under study is the production of an heavy $W^{\pm\prime}$ boson which decays into a single charged lepton plus missing transverse energy. For both the use of integral and differential charge asymmetries we are also developing quantitative estimates of their sensitivity through appropriate confidence levels.

1. Introduction

Contrarily to most of the previous high energy particle colliders, the LHC is a charge asymmetric machine. For charged final states, denoted $FS^{\pm}$, the integral charge asymmetry, denoted A_C, is defined by

$$A_C = \frac{N(FS^+) - N(FS^-)}{N(FS^+) + N(FS^-)} \tag{1}$$

where $N(FS^+)$ and $N(FS^-)$ represent respectively the number of events bearing a positive and a negative charge in the FS. Practically, we defined the charged final states as event topologies containing an odd number of high p_T charged and isolated leptons within the fiducial volume of the detector. For a $FS^{\pm}$ produced at the LHC in $p+p$ collisions, this quantity is positive or null, whilst it is always compatible with zero for a $FS^{\pm}$ produced at the TEVATRON in $p+\bar{p}$ collisions.

Let's consider the Drell-Yan production of $W^{\pm}$ bosons in $p+p$ collisions in order to illustrate the $A_C(\ell^{\pm})$ observable. We added the $(\ell^{\pm})$ to A_C to specify that we use the lepton charged asymmetry, not directly that of the $W^{\pm}$ boson. It is obvious for this simple $2 \to 2$ s-channel process that more W^+ than W^- are produced. Indeed, denoting y_W the rapidity of the W boson, the corresponding range of the Björken x's: $x_{1,2} = \frac{M_{W^{\pm}}}{\sqrt{s}} \times e^{\pm y_W}$, probe the charge asymmetric valence parton densities within the proton. This results in having more $U + \bar{D} \to W^+$ than $\bar{U} + D \to W^-$ configurations in the initial state (IS). Here U and D collectively and respectively represent the up and the down quarks. For the $W^{\pm} \to \ell^{\pm}\nu$ inclusive process, the dominant contribution to $A_C(\ell^{\pm})$ comes from the difference in rate between the $u+\bar{d}$ and the $d+\bar{u}$ quark currents in the IS. Using the usual notation $f(x, Q^2)$ for the parton density functions (PDF) and within the leading order (LO) approximation, this can be expressed as:

$$A_C(\ell^{\pm}) \approx \frac{u(x_{1,2}, M_W^2)\bar{d}(x_{2,1}, M_W^2) - \bar{u}(x_{1,2}, M_W^2)d(x_{2,1}, M_W^2)}{u(x_{1,2}, M_W^2)\bar{d}(x_{2,1}, M_W^2) + \bar{u}(x_{1,2}, M_W^2)d(x_{2,1}, M_W^2)} \tag{2}$$

where the squared four-momentum transfer Q^2 is set to M_W^2.

2. Indirect Mass Measurements

2.1. Relation Between Mass and Integral Charge Asymmetry

From equation 2, we can see that the Q^2 evolution of the parton density functions (PDFs) govern the Q^2 evolution of $A_C(\ell^{\pm})$. The former are known, up-to the NNLO in QCD, as solutions of the DGLAP equations [2]. One could therefore think of using an analytical functional form to relate $A_C(\ell^{\pm})$ to the squared mass of the s-channel propagator, here M_W^2. However there are additional contributions to the $W^{\pm}$ inclusive production. At the Born level, some come from other flavour combinations in the IS of the s-channel, and some come from the u and the t-channels. On top of this, there are higher order corrections. These extra contributions render the analytical expression of the Q^2 dependence of $A_C(\ell^{\pm})$ much more complicated. Therefore we choose to build process-dependent numerical mass template curves for $A_C(\ell^{\pm})$ by varying $\mathrm{M}_{FS^{\pm}}$. These mass templates constitute inclusive and flexible tools into which all the above-mentioned contributions to $A_C(\ell^{\pm})$ can be incorporated, they can very easily be built within a restricted domain of the signal phase space imposed by kinematic cuts.

In section 2 of this proceedings we exploit the $A_C(\ell^{\pm})$ to set a new type of constraint on the mass of the charged $FS^{\pm}$. In section 3, we present preliminary results on the use of $A_C(\ell^{\pm})$ as a new discriminating observable between a signal and its background processes.

We separate section 2 into two parts. The first one, in sub-section 2.2, is dedicated to present in full length the method of indirect mass measurement that we propose on a known Standard Model (SM) process. We choose the $W^{\pm} \to \ell^{\pm} + \not{E}_T$ inclusive production at the LHC to serve as a test bench. In the second part of section 2, in sub-section 2.3, we repeat the method on a "Beyond the Standard Model" (BSM) process. We choose a SUSY search process of high interest, namely $\tilde{\chi}_1^{\pm} + \tilde{\chi}_2^0 \to 3\ell^{\pm} + \not{E}_T$. For both the SM and the BSM processes, we obviously tag the sign of the FS by choosing a decay into one (or three) charged lepton(s) for which the sign is experimentally easily accessible.

2.2. A Standard Model Test Bench Process

2.2.1. Theoretical Prediction of $A_C(W^{\pm} \to \ell^{\pm}\nu)$

The theoretical $A_C(\ell^{\pm})$ raw (LHS) and fitted (RHS) template curves for the MRST2007lomod PDF are displayed in Fig. 1. For the raw template curve, the breakdown of the theory uncertainties are displayed as colored bands. We note the evolution of $A_C(\ell^{\pm})$ as a function of the artificially varied $W^{\pm}$ mass is a monotonic increasing function that can be described by a polynomial of logarithms of the logarithm of $M_{W^{\pm}}$: $A_C[M_{W^{\pm}}] = \sum_{i=0}^{N} A_i \times [Log[Log[M_{W^{\pm}}]]]^i$. This functional form is inspired by a parametrization of the analytical solution of the DGLAP non-singlet equation.

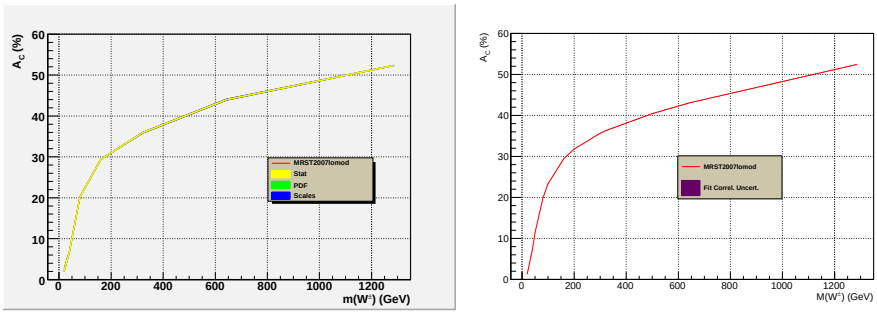

Figure 1. Theoretical $A_C(\ell^{\pm})$ raw (LHS) and fitted (RHS) template curves for the MRST2007lomod PDF.

2.2.2. Experimental Measurement of $A_C(W^{\pm} \to \ell^{\pm}\nu)$

In this subsection we extract $A_C(W^{\pm} \to \ell^{\pm}\nu)$ in presence of some background processes. To this end we generate Monte Carlo samples for the signal and the background processes in p+p colissions at $\sqrt{s} = 7$ TeV with an integrated luminosity of $L = 1\ fb^{-1}$. We use the MRST2007lomod [3] as the default parton density function (PDF) here and in all reported studies hereafter. We use a fast simulation of the response of the ATLAS detector. And we apply some selection cuts to optimize the signal to noise ratio. We keep the events with a hard and isolated electron or muon that has a $p_T > 25$ GeV. These events must have a missing transverse energy larger than 25 GeV and a transverse mass larger than 40 GeV. The corresponding efficiencies, events yields and expected charge asymmetries reported in Tab. 1.
After applying the above event selection, the A_C of all surviving events has two experimenal biases. One of these biases comes from the selection cuts on the lepton kinematics, the other one comes from the background contamination. The former bias is encoded in the experimental template and not corrected for. In order to correct for the latter experimenal bias, we apply a background subtraction which relies upon the following equation:

$$A_C^{Exp}(S) = (1 + \alpha^{Exp}) \cdot A_C^{Exp}(S + B) - \alpha^{Exp} \cdot A_C^{Exp}(B) \tag{3}$$

where $\alpha^{Exp} = \frac{N_B^{Exp}}{N_S^{Exp}}$ is the noise (B) to signal (S) ratio. We also use this equation to propagate the experimental systematic uncertainties into $A_C^{Exp}(S)$ accounting for the correlations between α^{Exp}, $A_C^{Exp}(B)$, and $A_C^{Exp}(S + B)$. In this notation "Exp" stands for expected from the Monte Carlo (MC) simulation.
This procedure enables to obtain $A_C^{Meas}(S)$ starting from $A_C^{Exp}(S)$ where "Meas" stands for measured and represents $A_C(S)$ after the background subtraction and the propagation of the

Process	ϵ (%)	N_{exp} (k evts)	$A_C \pm \delta A_C^{Stat}$ (%)
Signal: $W^{\pm} \to e^{\pm}\nu_e$			
$M(W^{\pm}) = 40.2$ GeV	0.81 ± 0.01	290.367	9.66 ± 1.57
$M(W^{\pm}) = 60.3$ GeV	13.69 ± 0.05	2561.508	11.22 ± 0.38
$M(W^{\pm}) = \underline{80.4}$ GeV	29.59 ± 0.04	3343.195	16.70 ± 0.18
$M(W^{\pm}) = 100.5$ GeV	39.19 ± 0.07	2926.093	20.77 ± 0.22
$M(W^{\pm}) = 120.6$ GeV	44.84 ± 0.07	2357.557	23.19 ± 0.21
$M(W^{\pm}) = 140.7$ GeV	48.66 ± 0.07	1899.820	25.29 ± 0.20
$M(W^{\pm}) = 160.8$ GeV	51.28 ± 0.07	1527.360	26.87 ± 0.19
$M(W^{\pm}) = 201.0$ GeV	54.54 ± 0.07	1.032	29.06 ± 0.18
Background	-	91.614 ± 1.706	10.07 ± 0.15
$W^{\pm} \to \mu^{\pm}\nu_{\mu}/\tau^{\pm}\nu_{\tau}/q\bar{q}\prime$	0.211 ± 0.003	71.350	12.92 ± 1.25
$t\bar{t}$	5.76 ± 0.02	6.600	1.00 ± 0.37
$t + b,\ t + q(+b)$	3.59 ± 0.01	1.926	28.97 ± 0.35
$W + W,\ W + \gamma^*/Z,\ \gamma^*/Z + \gamma^*/Z$	2.94 ± 0.01	2.331	10.65 ± 0.35
$\gamma + \gamma,\ \gamma + jets,\ \gamma + W^{\pm},\ \gamma + Z$	0.201 ± 0.001	0.759	17.25 ± 0.53
γ^*/Z	0.535 ± 0.001	5.746	4.43 ± 0.23
QCD HF	$(0.44 \pm 0.17) \times 10^{-4}$	1.347	14.29 ± 37.41
QCD LF	$(0.87 \pm 0.33) \times 10^{-4}$	1.555	71.43 ± 26.45

Table 1. Selection efficiencies, event yields and expected integral charge asymmetries for the $W^{\pm} \to e^{\pm}\nu_e$ analysis.

experimental systematic uncertainties. The evolution of $A_C^{Meas}(S)$ with respect to $M_{W^{\pm}}$ enables to construct experimental $A_C(\ell^{\pm})$ template curves. This is illustrated for the electron channel in Fig. 2.

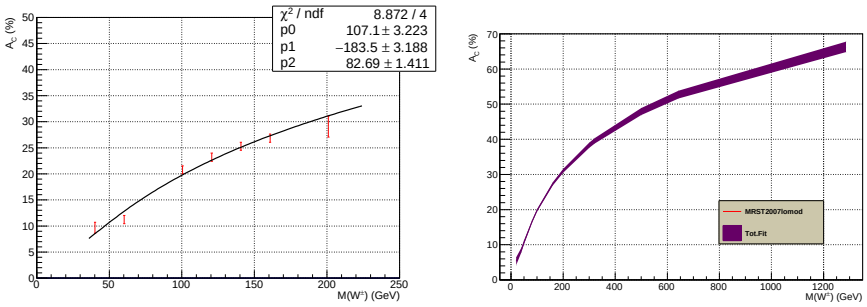

Figure 2. The A_C^{Meas} raw (LHS) and fitted (RHS) template curves for the electron channel.

2.2.3. Indirect Determination of $M_{W^{\pm}}$

The measured $A_C(\ell^{\pm})$ from the electron and the muon channels are converted into $M_{W^{\pm}}$ estimtates using the corresponding experimental templates.

- $A_C^{Meas.Fit}(S) = (16.70 \pm 0.35)\% \Rightarrow M^{Meas.Fit}(W^{\pm} \to e^{\pm}\nu_e) = 81.08^{+2.06}_{-2.01}$ GeV
- $A_C^{Meas.Fit}(S) = (17.52 \pm 0.18)\% \Rightarrow M^{Meas.Fit}(W^{\pm} \to \mu^{\pm}\nu_{\mu}) = 79.67^{+3.56}_{-1.39}$ GeV

These two indirect mass measurements are then combined through a weighted mean: $M^{Comb.Meas.}(W^{\pm}) = 80.30 \pm 0.96$ (Exp.Comb.) GeV. The theoretical template curve is read-up at the central value of the estimated $M_{W^{\pm}}$ and the corresponding uncertainties $^{+0.19}_{-0.21}$ GeV are summed in quadrature with the experimental ones so as to give the total uncertainties:

$$M_{W^{\pm}} = 80.30^{+0.98}_{-0.98}\ (\text{MRST2007lomod})\ \ \text{GeV}. \tag{4}$$

2.3. A SUSY Physics Case

Here we apply the previous method to a SUSY "golden channel": $p + p \to \tilde{\chi}_1^{\pm} + \tilde{\chi}_2^0 \to 3\ell^{\pm} + \not{E}_T$.

2.3.1. Theoretical Prediction of $A_C(\tilde{\chi}_1^{\pm} + \tilde{\chi}_2^0)$

The theoretical $A_C[M_{\tilde{\chi}_1^{\pm}} + M_{\tilde{\chi}_2^0}]$ raw (LHS) and fitted (LHS) template curves for the MRST2007lomod PDF are displayed in Fig. 3. The fit functional form is analogous to that of section 2: $A_C[M_{\tilde{\chi}_1^{\pm}} + M_{\tilde{\chi}_2^0}] = \sum_{i=0}^{N} A_i \times [Log[Log[M_{\tilde{\chi}_1^{\pm}} + M_{\tilde{\chi}_2^0}]]]^i$.

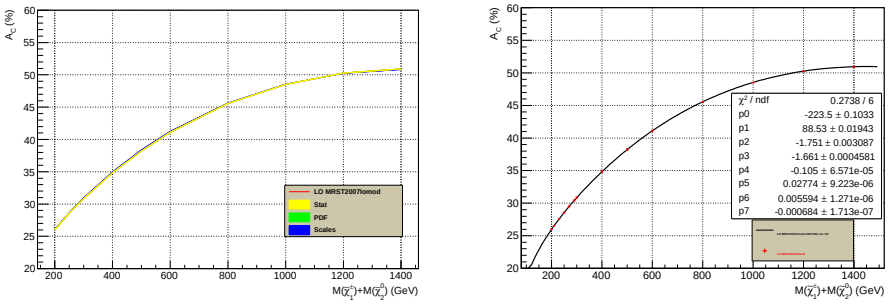

Figure 3. Theoretical A_C raw (LHS) and fitted (RHS) template curves for the MRST2007lomod PDF.

2.3.2. Experimental Measurement of $A_C(\tilde{\chi}_1^{\pm} + \tilde{\chi}_2^0 \to 3\ell^{\pm} + \not{E}_T)$

In this subsection we generate Monte Carlo samples for the signal and the background processes in p+p colissions at $\sqrt{s} = 8$ TeV with an integrated luminosity of $L = 20\ fb^{-1}$. Two different types of SUSY spectra are considered. First, there's one, denoted S1 signal, where sleptons have masses intermediate between $M_{\tilde{\chi}_2^0}$ (set equal to $M_{\tilde{\chi}_1^{\pm}}$) and $M_{\tilde{\chi}_1^0}$. Second, there's another, denoted S2 signal, where sleptons have masses much larger than $M_{\tilde{\chi}_2^0} = M_{\tilde{\chi}_1^{\pm}}$. Again, we use a fast simulation of the response of the ATLAS detector. And we apply some selection cuts to optimize the signal to noise ratio. We keep the events with three hard and isolated leptons (electrons and/or muons) that have a $p_T > 20, 10, 10$ GeV. These events must have a missing transverse energy larger than 35 GeV and a stransverse mass, M_{T2} [4][5], larger than 75 GeV. The A_C background subtraction is applied, the experimental uncertainties are propagated into A_C^{Meas} from which experimental template curves are derived. A_C^{Meas} are converted into estimated sums of masses: $M_{\tilde{\chi}_1^{\pm}} + M_{\tilde{\chi}_2^0}$ with the same treatment of the experimental and theoretical uncertainties than in section 2.2.1.

2.3.3. Indirect Determination of $M_{\tilde{\chi}_1^{\pm}} + M_{\tilde{\chi}_2^0}$

As in sub-section 2.2.3, the A_C^{Meas} can be translated into estimates of $M_{\tilde{\chi}_1^{\pm}} + M_{\tilde{\chi}_2^0}$. Closure tests displayed in Fig. 4 illustrate the quality (linearity, abscence of offset and uncertainty) of these indirect mass measurements, especially in the mass ranges with high signal sensitivities (above 5σ for S1 and above 3σ for S2) which are highlighted.

2.3.4. Results

The accuracy of the indirect mass measurements for the W mass is better than 2%, and it is better than 6% for the S1 and S2 chargino-neutralino signal samples within their mass range of high sensitivity.

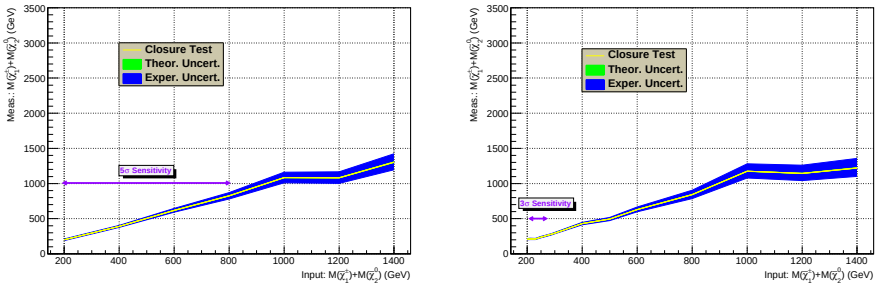

Figure 4. Closure tests for the indirect measurements of $M_{\tilde{\chi}_1^\pm} + M_{\tilde{\chi}_2^0}$ for S1 (LHS) and S2 (RHS) signal samples.

3. Improved Discrimination Between Signal and Background

In the context of BSM searches, the method of indirect mass measurement presented in section 2 can only be utilized after a significant excess of a signal produced through a charged current is discovered. This raises the following question: could the charge asymmetry observable be used in the BSM search itself? Our answer is yes, and to illustrate this we choose an exotic physics case which is the search for an additional charged electroweak boson: $p+p \to W^{\pm\prime} \to 1\ell^\pm + \not{E}_T$.

3.1. Search in the Muon Channel

More precisely, we recast an ATLAS Run 2 analysis [6] just in the muon channel so far.

3.1.1. MC Samples and Detector Simulation

MC samples are generated for the signal using Pythia 8.157 [7] and for the background processes using Herwig++ 2.5.2 [8] and Alpgen 2.14 [9] (interfaced to Pythia v8.157 for the parton shower, the hadronization and the decays). For the signal, the following mass hyoptheses are considered: $M_{W^{\pm\prime}} = 1, 2, 3, 4$ TeV. All these MC samples are produced for $p+p$ collisions at $\sqrt{s} = 8$ TeV and normalized to an integrated luminosity of L=20 fb^{-1}.

3.1.2. Event Selection

The response of the ATLAS detector is crudely simulated by Delphes 3.3.2 [10]. In order to extract the signal from the background processes, we select events with one isolated muon, with $p_T(\mu^\pm) > 45$ GeV and $|\eta(\mu^\pm)| < 2.4$. Most of the background processes are suppressed by requiring $\not{E}_T > 45$ GeV and especially $M_T = \sqrt{2p_T(\mu^\pm)\not{E}_T(1 - cos\Delta\phi)} > 800$ GeV. After these cuts are applied, the resulting selection efficiencies, event yields and expected integral charge asymmetries are compiled within Tab. 2.
In the ATLAS analysis, the final discriminant is the high M_T tail (beyond 800 GeV). Instead, in our selection, the final discriminant is $A_C(\ell^\pm)$.

3.1.3. Systematic Uncertainties

The theoretical uncertanties are due to the unknown QCD scales for fixed order (here leading order) $A_C(\ell^\pm)$ calculations and to the PDF$\oplus\alpha_S$ uncertainties. The latter are calculated using the PDF4LHC15_nlo_mc_pdfas set [11][12][13][14] and following the PDF4LHC recommendations for the LHC Run 2 [15]. This is implemented using the LHAPDF 6.1.5 [16] interface.
For the experimental uncertainties, we use those quoted in Ref. [6]:

- $\not{E}_T$ scale & resolution: 0.1% (S), 0.5% (B)

Process	ϵ (%)	N_{exp} (evts)	$A_C \pm \delta A_C^{Stat}$ (%)
Signal: $W^{\pm\prime} \to \mu^{\pm}\nu_\mu$			
$M(W^{\pm\prime}) = 1$ TeV	36.36 ± 0.07	8561.59	48.56 ± 0.94
$M(W^{\pm\prime}) = 2$ TeV	64.04 ± 0.07	317.23	60.61 ± 4.47
$M(W^{\pm\prime}) = 3$ TeV	42.87 ± 0.07	12.53	60.48 ± 22.50
$M(W^{\pm\prime}) = 4$ TeV	21.15 ± 0.06	1.33	57.28 ± 71.04
Background	-	5.91	1.30 ± 41.14
$W^{\pm} \to \mu^{\pm}\nu_\mu/\tau^{\pm}\nu_\tau/q\bar{q}\prime + LF$	0.00 ± 0.00	0.00	–
$W^{\pm} \to \mu^{\pm}\nu_\mu/\tau^{\pm}\nu_\tau/q\bar{q}\prime + HF$	$5.28 \times 10^{-4} \pm 1.21 \times 10^{-5}$	1.78	82.51 ± 42.32
$t\bar{t}$	0.00 ± 0.00	0.00	–
$t + b,\ t + q(+b)$	0.00 ± 0.00	0.00	–
VV	$4.09 \times 10^{-4} \pm 1.14 \times 10^{-5}$	1.65	-100.00 ± 0.00
VVV	$5.41 \times 10^{-3} \pm 4.47 \times 10^{-5}$	2.28×10^{-2}	6.85 ± 8.26
$\gamma + \gamma,\ \gamma + jets,\ \gamma + W^{\pm},\ \gamma + Z$	0.00 ± 0.00	0.00	–
$\gamma^*/Z + LF$	$6.97 \times 10^{-2} \pm 3.71 \times 10^{-5}$	2.45	-87.15 ± 46.67
$\gamma^*/Z + HF$	0.00 ± 0.00	0.00	–
QCD HF	0.00 ± 0.00	0.00	–
QCD LF	0.00 ± 0.00	0.00	–

Table 2. Selection efficiencies, event yields and expected integral charge asymmetries for the $W^{\pm\prime} \to \mu^{\pm}\nu_\mu$ analysis.

- Lepton energy/momentum scale & resolution: 2.3% (S), 18.1% (B)

Process	$\delta A_C^{Stat} \oplus \delta A_C^{Syst}$ (B)	$\delta A_C^{Stat} \oplus \delta A_C^{Syst}$ (S+B)
$M(W^{\pm\prime}) = 1$ TeV	–	1.74 %
$M(W^{\pm\prime}) = 2$ TeV	–	9.83 %
$M(W^{\pm\prime}) = 3$ TeV	–	161.89 %
$M(W^{\pm\prime}) = 4$ TeV	–	41.31 %
Background	3.88%	–

Table 3. Total uncertainties for the S and S+B hypotheses.

Note that the very large uncertainty for $M_{W^{\pm\prime}} = 3$ TeV: $\delta A_C^{Stat} \oplus \delta A_C^{Syst} = 161.89\%$ comes from a few unphysical outlier weights in the computation of the PDF uncertainty obtained through a PDF reweighting. For the sake of being over-conservative, we left it as is in the limit calculation, though obviously it should be capped to 100% to actually make sense.

3.1.4. Statistical Interpretation

In order to distinguish the (S) and (B) hypotheses, standard log. likelihood ratios were computed and used as test statistics Q following the formalism in Ref. [17]. Their distributions, including the total uncertainties, are shown in Fig. 5, in blue and in red for the (B) and the (S+B) hypotheses, respectively.

By integrating the test statistics distributions below or beyond Q_B^{Med}, we calculate each hypothesis p-value and consequently the signal confidence level CL_S. This enables to calculate the 95% C.L. exclusion limits for the different signal mass hypotheses, as shown in Fig 6.

3.1.5. Result

Here are the respective 95% C.L. exclusion limits obtained by the ATLAS analysis and with our method:

$$M_{W^{\pm\prime}} > 2.97 \text{ TeV } (\mathrm{M_T - tail}) \tag{5}$$

$$M_{W^{\pm\prime}} > 3.0 \text{ TeV } (\mathrm{A_C}) \tag{6}$$

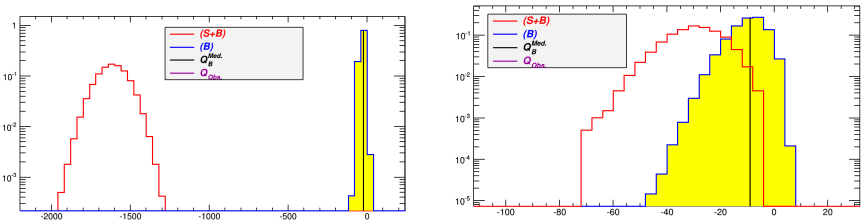

Figure 5. Distribution of the tests statistics for a $W^{\pm\prime}$ mass of 2 TeV (LHS) and 3 TeV (RHS).

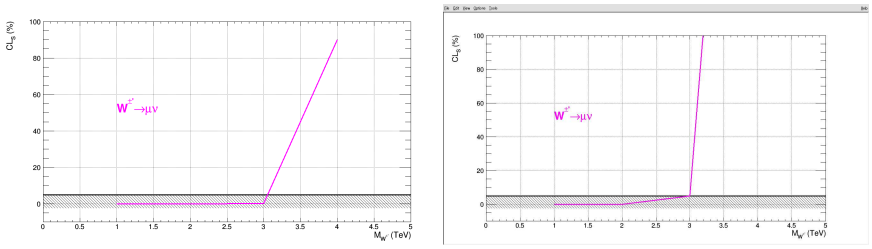

Figure 6. Confidence levels with (bottom) and without (top) the systematics uncertainties.

This preliminary result shows that our new method based upon A_C has a sensitivity equivalent to that of the state-of-the-art method.

3.2. Acknowledgments

The author would like to thank to following persons for useful discussions regarding the calculations of the confidence levels reported in sub-section 3.1.4: F. James, A. Tilquin, K. Cranmer, G. Cowan, and Y. Coadou.

References

[1] Muanza G S and Serre T 2016 *JHEP* **04** 179 (*Preprint* `arXiv:1412.6695`)
[2] Cafarella A, Coriano C and Guzzi M 2006 *Nucl. Phys.* **B748** 253–308 (*Preprint* `hep-ph/0512358`)
[3] Sherstnev A and Thorne R S 2008 *Eur. Phys. J.* **C55** 553–575 (*Preprint* `0711.2473`)
[4] Polesello G and Tovey D R 2010 *JHEP* **03** 030 (*Preprint* `0910.0174`)
[5] Tovey D URL `http://projects.hepforge.org/mctlib`
[6] Aad G *et al.* (ATLAS) 2014 *JHEP* **09** 037 (*Preprint* `1407.7494`)
[7] Sjostrand T, Mrenna S and Skands P Z 2008 *Comput. Phys. Commun.* **178** 852–867 (*Preprint* `0710.3820`)
[8] Gieseke S, Grellscheid D, Hamilton K, Ribon A, Richardson P, Seymour M H, Stephens P and Webber B R 2006 (*Preprint* `hep-ph/0609306`)
[9] Mangano M L, Moretti M, Piccinini F, Pittau R and Polosa A D 2003 *JHEP* **07** 001 (*Preprint* `hep-ph/0206293`)
[10] de Favereau J, Delaere C, Demin P, Giammanco A, Lematre V, Mertens A and Selvaggi M (DELPHES 3) 2014 *JHEP* **02** 057 (*Preprint* `1307.6346`)
[11] Carrazza S, Latorre J I, Rojo J and Watt G 2015 *Eur. Phys. J.* **C75** 474 (*Preprint* `1504.06469`)
[12] Gao J and Nadolsky P 2014 *JHEP* **07** 035 (*Preprint* `1401.0013`)
[13] Dulat S, Hou T J, Gao J, Guzzi M, Huston J, Nadolsky P, Pumplin J, Schmidt C, Stump D and Yuan C P 2016 *Phys. Rev.* **D93** 033006 (*Preprint* `1506.07443`)
[14] Harland-Lang L A, Martin A D, Motylinski P and Thorne R S 2015 *Eur. Phys. J.* **C75** 204 (*Preprint* `1412.3989`)
[15] Butterworth J *et al.* 2016 *J. Phys.* **G43** 023001 (*Preprint* `1510.03865`)
[16] Buckley A e a 2015 *Eur. Phys. J.* **C75** 132 (*Preprint* `1412.7420`)
[17] Cowan G 2013 (*Preprint* `1307.2487`)